# Testing of hydraulically driven ramming device

JIRI BALLA, ZBYNEK KRIST, CONG ICH LE
Department of weapons and ammunition
University of Defence
Kounicova 65, 662 10 Brno
CZECH REPUBLIC
jiri.balla@unob.cz, zbynek.krist@unob.cz, congich.le@unob.cz, http://www.unob.cz

*Abstract:* - The purpose of this article is to familiarize with new attitude to finding technical characteristics of the hydraulic powered ramming devices used in heavy guns. The results are values of the input and output pressures, input and output flows, temperature in hydraulic oil. The damping coefficient, and hydraulic resistances in the hydraulic circuits are derived from own technical experiments. The kinematic and dynamic parameters, as are the ramming velocity, the ramming force, and the ramming power, are derived from the measured input and output flows of the linear hydraulic actuator. They enable to give expert opinion about ramming device operation as whole. The results are used for validation of the dynamic model of the ramming device, and they serve as input data in course of calculation when is operating. Finally, results can be used as diagnostics data of the loading systems, and whole procedure as an example of the practicable technique in the higher military repair units because the current methods based on the military directives use the time of operation cycle as one and only diagnostics parameter.

*Key-Words:* - Flowmeter, Pressure Gauge, Ramming Device, Ramming Velocity, Temperature of Fluid.

## 1 Introduction

The ramming device is one of the most important parts of the entire loading device. The function of each part can be explained by the so-called functional diagram. This functional diagram is a graph of the dependencies of the displacement of individual subsystems in time. An example of this functional diagram belonging to the loading system for a gun utilizing the separate ammunition is in Fig. 1, see [1].

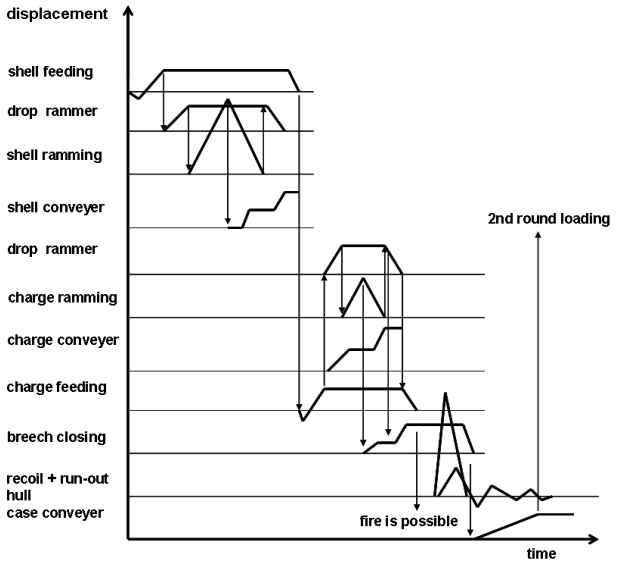


Fig. 1

The functional diagram consists of eleven curves belonging to different subsystems or to different periods of the loading cycle. Time is represented by the horizontal axis and individual displacements are drawn in the vertical direction. The ramming device used in this case study is one of the parts of the whole loading system, beginning operation after the shell (projectile) or charge feeding, see [2]. The ramming device is mostly common for projectiles and charges stored in cases.

In the past ramming devices parameters were determined only from the falling back of projectile point of view. In addition, only the duration of each operation were monitored, see [3]. The hydraulic computational models with lumped parameters, see [4], [5], required to establish a number of input parameters that are not available from equipment manufacturers, or available literature deals with a narrow range of facilities whose results cannot be extended to other installations. Generally, the problem is to find corresponding input parameters for calculations, or published results have a very limited range of applicability constants, see [6]. They are mainly the values of hydraulic capacities, hydraulic resistances, and damping coefficients in hydraulic drives. Contemporary measurement tools enable to establish parameters as ramming velocity and ramming force according to acknowledged standards, see [7]. Moreover, there presented measuring system allows after appropriate software analysis to determine the hydraulic characteristics needed for model calculations and defect simulations.

## 2 Problem Formulation

The ramming device, outgoing from the structure scheme in Fig. 2, uses the linear hydraulic motor, where its $v_R$ piston rod velocity depends on the $Q_1$ input flow, and the $S_1$ input piston area according to the relation

$$v_R = \dot{x}_1 = \frac{Q_1}{S_1} . \quad (1)$$

Same value can be determined using the output flow according to the similar equation

$$v_R = \dot{x}_1 = \frac{Q_2}{S_2} . \quad (2)$$

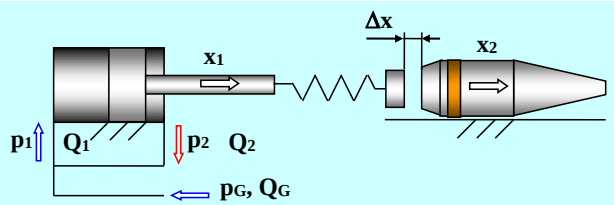


Fig. 2

The input flow is given by the algebraic equation

$$Q_1 = Q_G + Q_2 , \quad (3)$$

where

$Q_G$ - the source flow from generator,

$Q_2$ - output flow.

The $x_2$ coordinate belongs to the shell (projectile) displacement.

The mechanical system equations are written according to Fig. 2 in the following way suitable for calculation, see [2], [5]:

$$\begin{aligned} m_1\ddot{x}_1 &= F_{RAM} + k_{RAM}(x_2 - x_1) - F_D \\ m_2\ddot{x}_2 &= -k_{RAM}(x_2 - x_1) - F_f \end{aligned} , \quad (4)$$

where

$F_D$ – the damping force depends on the piston velocity and damping coefficient,

$F_f$ – the friction force acting against the projectile motion, depending on the elevation angle.

The flexible linkage is modelled by a spring with the linear stiffness $k_{RAM}$ between the projectile and the chain rammer, there represented by the reduced linear stiffness of the hydraulic motor piston rod and the rammer chain.

The projectile is rammed by the ramming force depending on the $p_1$ input pressure and $p_2$ output pressure according to the following equation

$$F_{RAM} = p_1 S_1 - p_2 S_2 , \quad (5)$$

where

$S_2$ – output effective area of the piston.

The input and output connection in Fig. 2 for the linear hydraulic motors is known as asymmetrical used to reach the required ramming velocity at the end of the projectile movement. A small clearance Δx of some tens of millimeters is included before the beginning of the projectile motion when the rammer is accelerated. Afterwards both projectile and rammer move together or due to the $k_{RAM}$ limited rigidity of both parts oscillatory movement arises. After projectile inserting into the barrel with the minimal velocity 0.3 m/s so it does not fall back it has to be engraved by means of its driving band into the barrel forcing cone, see Fig. 3, and [4]. The maximal velocity is limited to 6.5 m/s due to the fuse safety and aligning of the axis projectile with the bore axis.

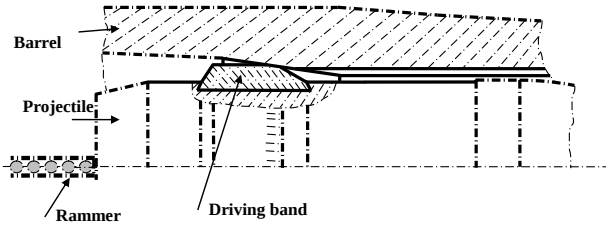


Fig. 3

The pressures $p_1$ and $p_2$ are given based on the scheme of the hydraulic circuit in Fig. 2 and follow from the flow continuity equations, see [4]. The differential equations of the first order are:

$$\begin{aligned} \frac{dp_1}{dt} &= \frac{(Q_1 - S_1\dot{x}_1 - Z_1 p_1)}{C_1} \\ \frac{dp_2}{dt} &= \frac{(S_1\dot{x}_1 - Q_2 - Z_2 p_2)}{C_2} \end{aligned} . \quad (6)$$

The input and output hydraulic capacities $C_1$, $C_2$ are given, see [4]:

$C_1 = C_{01} + \beta_L S_1 x_1$ – input hydraulic capacity,

$C_{01} = \beta_L V_{01} + \beta_H V_{H1}$,

$C_2 = C_{02} + \beta_L S_2 (h - x_1)$ – output hydraulic capacity,

$C_{02} = \beta_L V_{02} + \beta_H V_{H2}$,

$V_{01}$ – input liquid volume in the pipe, leading from distributor to input hose,

$V_{02}$ – output liquid volume in the pipe, leading from hydraulic motor to output hose,

$h$ – whole piston displacement,

$V_{H1}$ – input liquid volume in the hose, leading from input pipe to hydraulic motor,

$V_{H2}$ – output liquid volume in the hose, leading from hydraulic motor to output pipe,

$\beta_L$ – bulk modulus of the fluid

$\beta_H$ – hose volume compressibility factor,

$R_1$ – input hydraulic resistance,

$R_2$ – output hydraulic resistance,

$Z_1$ – input hydraulic leakage,

$Z_2$ – output hydraulic leakage.

The main characteristics of hydraulically powered ramming devices that are checked during technical inspections are the ramming velocity and the hydraulic pressures, see [7]. Next part describes how to determine these and derived ramming system parameters using of the new technical means.

## 3 Problem Solution

The five-channel measuring system scheme is shown in Fig. 4. Signals from sensors are amplified by means of the amplifiers MA-UI 5B. Afterwards they are processed by the data acquisition system USB-AD16f, and finally data are stored in PC. The 1000 Hz sampling frequency had been sufficient for this purpose. The experimental arrangement of the measuring chain in Fig 4 enables directly to set the following characteristics: $p_1$, $p_2$ input and output pressures, $Q_1$, $Q_2$ input and output flows, and the T liquid temperature during projectile ramming.

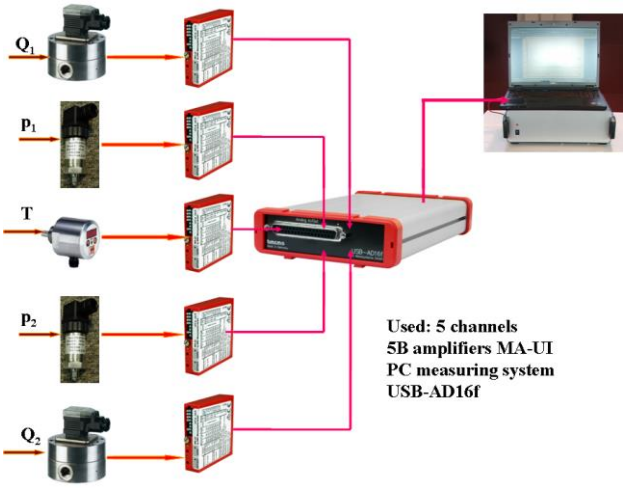


Fig. 4

The measurement system hardware consists of two pressure sensor/transducers, two flow transducers, and one hydraulic liquid temperature sensor. First of them are sensors measuring the input and output pressures, using of ceramic sensors element SEN-8700A 125 suitable for systems with high dynamic changes. These sensors located in the required places on the hydraulic houses have ranges up to 10 MPa, which is sufficient for maximal operation pressure 4 MPa. The flows have been measured by means of the gear wheel volume flow meters DZR with the range 1 liter per minute to 250 liters per minute. The resolution is 191 pulses per liter. It means that 1 pulse gives 0.0052 liters. These flowmeters have replaced the previously used turbine flowmeters because of better dynamic properties at the beginning of the operation. The fluid temperature T was determined by means of temperature gauge TDA-15H2. The KOBOLD technology was connected with the BMC measuring and NextView® software system, see [8].

## 4 Results

Firstly, the test without rammed projectile was performed at elevation angle 0° (only rammer is driven). The results of output hydraulic parameters without any corrections are represented in the Fig. 5. Only rammer is in operation, then $F_f = 0$, in (4).

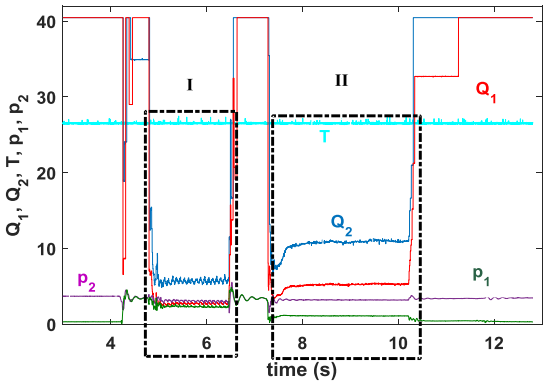


Fig. 5

The area I represents duration where the rammer inserts without the projectile into the barrel. Operation before is ramming device preparation when rammer drops into a position coaxial with the projectile axis and the barrel axis, see Fig. 1 as well. Afterwards the electrohydraulic distributor switches the fluid flow in the opposite direction and the rammer returns to the basic position. It is highlighted as area II. Flow units are the time between pulses in the millisecond units, pressures are in MPa.

The temperature of the hydraulic liquid during one cycle varies negligibly and can be considered constant, see Fig. 6, where there are depicted the original signal (magenta) and the signal after median and polynomial filtering (blue). In addition, random spikes of the voltage fluctuations and noise are also below the accuracy temperature sensor, which is ± 0.5 C.

The input and output flow charts depending on time are typified in Fig. 7. Unit of flow due to the small value is liter per second. Using (3) we get the desired flow of the generator during the insertion of the projectile. Only during this time hydraulic system operates in asymmetrical connection.

All flows are shown in Fig. 8. The hydraulic generator having the output flow approximately 60 l/min is able to deliver the required quantity of the hydraulic oil in time. The ramming time achieves 1.7 seconds.

Based on the results of measuring the flow rates can be estimated the rammer velocity using (1), (2), which maximal value achieves approximately 0.9 m/s. When the rammer moves back, the velocity lowers reaching 0.45 m/s. Then hydraulic system operates symmetrically.

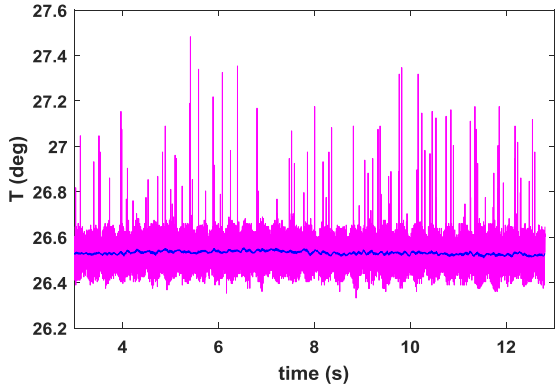


Fig. 6

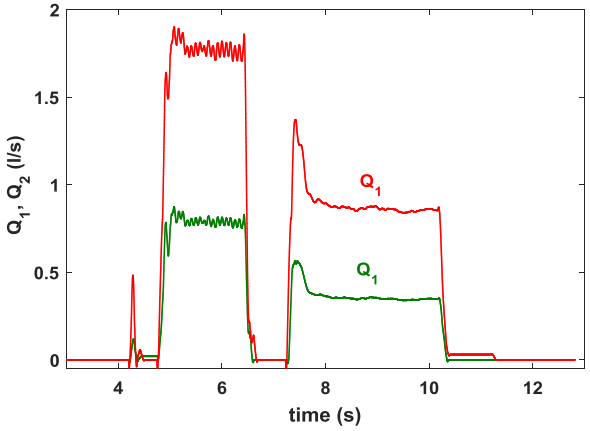


Fig. 7

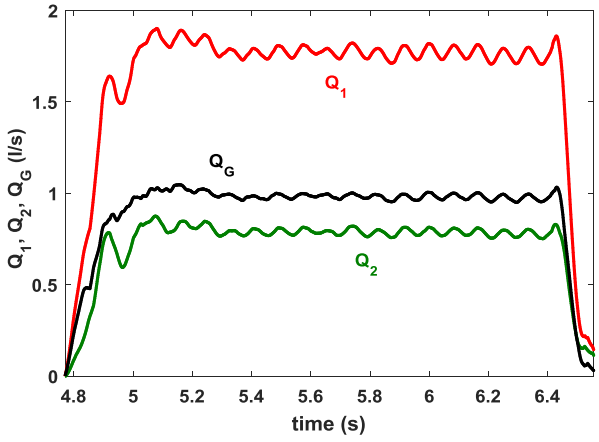


Fig. 8

The input and output pressures, see Fig. 9, enable to calculate derived parameters as are the ramming force, see (4), and the ramming power. Note, that the working pressure in the hydraulic system under examination device is set to 4 MPa, and during projectile insertion can operate the other hydraulically driven devices as conveyers, laying gears, etc.

The ramming force time history in Fig. 10 was calculated according to (4) and its mean value is approx. 1700 N. Due to the oscillation of the axial piston hydraulic generator the curve has similar course.

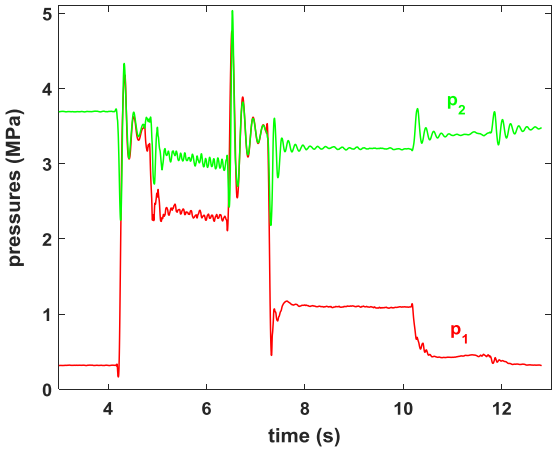


Fig. 9

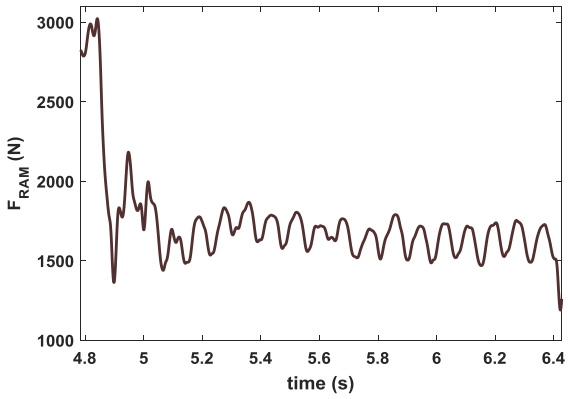


Fig. 10

The power of the ramming device calculated using formula

$$P = F_{\mathrm{RAM}} \cdot v_{\mathrm{RAM}}, \qquad (7)$$

is represented in Fig. 11, and supplemented by the ramming velocity $v_{\mathrm{RAM}}$.

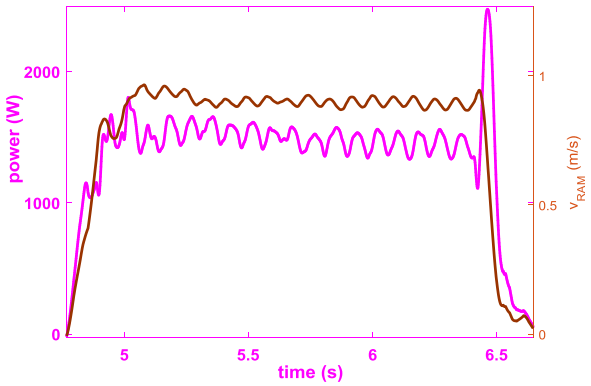


Fig. 11

The mean power achieves about 1450 W.
If we look at the first equation in (4), the coefficient of damping system $b_D$ can be obtained as a model value for real system according to literature, see [6] for example. The simplest method is to take into consideration linear dependence of the damping force on the piston rod velocity, as

$$F_D = b_D \cdot v_{RAM}. \tag{8}$$

The mean value during stable state is 1900 (N·s/m).
The ramming power and the rammer velocity when the rammer is moving back is shown in Fig. 12.

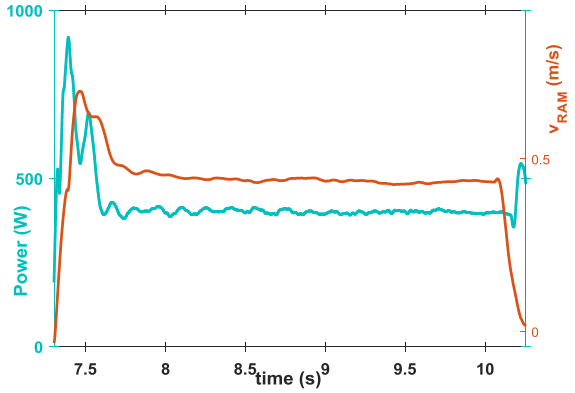


Fig. 12

The estimation of the hydraulic resistances for input and output circuits can be set using of the stable state equations, see [4], [5], [6]

$$Q_1 = \operatorname{sgn}(p_G - p_1)\sqrt{\frac{|p_G - p_1|}{R_1}}, \qquad Q_2 = \operatorname{sgn}(p_2 - p_1)\sqrt{\frac{|p_2 - p_1|}{R_2}}. \tag{9}$$

After rearrangements and excluding of the resistances $R_1$ and $R_2$ from (9), we get an estimation of the hydraulic resistances of the input and output parts as follows:
$R_1 = 2.2\text{x}10^{11}$ Pa·s$^2$·m$^6$, $R_2 = 1.14\text{x}10^{12}$ Pa·s$^2$·m$^6$.
When the ramming device inserts the projectile, the main characteristics follow in next figures. The course of the ramming velocity in Fig. 13 is similar to in Fig. 11. The ramming force in Fig. 14 increased over several tens newton compared with idling operation in Fig. 10.
Like the ramming force in the previous picture also the ramming power in Fig. 15, as compared with idling operation, has more oscillating course due to the weight of the projectile on a flexible chain rammer.

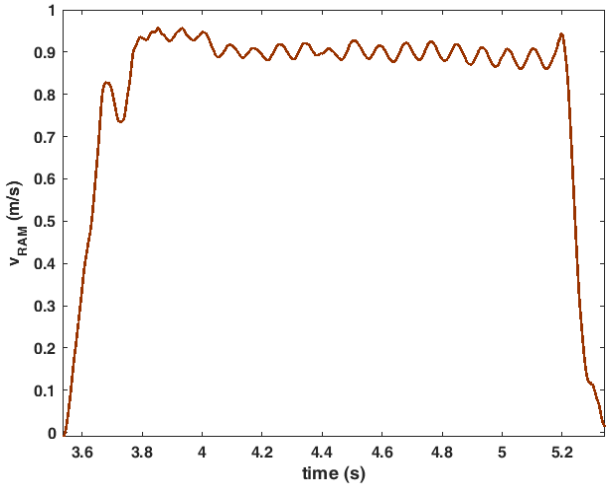


Fig. 13

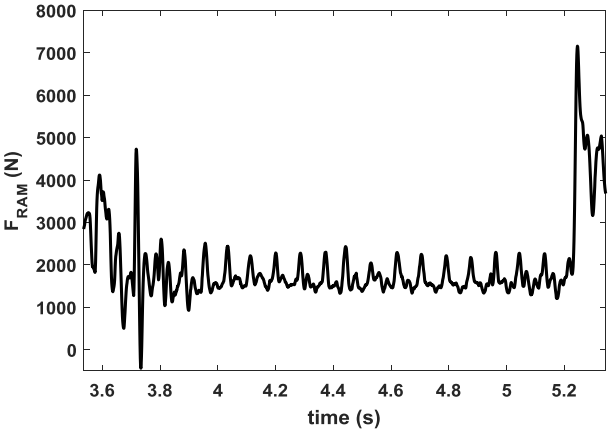


Fig. 14

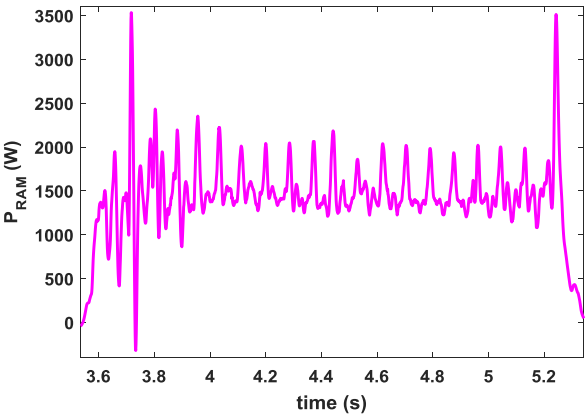


Fig. 15

Examples of the $\frac{dp_1}{dt}$, $\frac{dp_2}{dt}$ time-history diagrams in Fig. 16 enable to consider an introduction of the hydraulic capacities in calculations. The hydraulic capacities in (6) primarily influenced by pressure derivative course at the beginning and at the end of the movement. Then their effect is negligible and

significantly influence the course of the pressure when the system starts, stops or reverses.

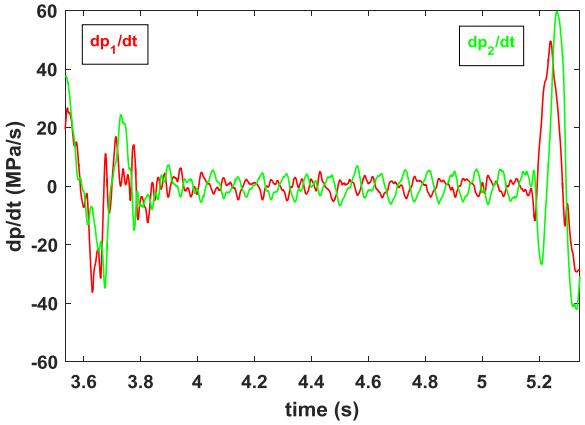


Fig. 16

## 5 Conclusion

A novel measurement procedure of parameters determination in the gun ramming devices with hydraulic drives has been described. The parameters needed for technical inspections according to the Directive [3] are in the first three lines of the Table I.

Table I Parameters of hydraulic ramming device

| Symbol | Quantity | Value |
|---|---|---|
| $t_{idle}$ | idle ramming device cycle time | 1.7 s |
| $t_{idle\text{-}back}$ | idle-back ramming device cycle time | 2.9 s |
| $t_{projectile}$ | projectile ramming cycle time | 1.8 s |
| $b_D$ | damping coefficient of system | 1900 N·s/m |
| $R_1$ | input hydraulic resistance | $2.2 \times 10^{11}$ Pa·s$^2$·m$^6$ |
| $R_2$ | output hydraulic resistance | $1.14 \times 10^{12}$ Pa·s$^2$·m$^6$ |

The other hydraulic parameters mentioned in the article are those that will be introduced in the new methodology of the technical inspections, similar to in [9]. They are mainly steady state inlet and outlet pressures $p_1$, $p_2$, together with the corresponding flow rates $Q_1$ and $Q_2$. These signals are used as reference signals for diagnostic purposes. In addition, the results will be used for calculations during simulations of ramming device since system is to be upgraded and retrofitted in order to improve its combat performance parameters. It has to include the cutting of the driving band of projectiles into the barrel bore forcing cone as it is detailed in [1] or [10], for example.

*References:*

[1] Balla, J., S. Jankovych, R., Duong, V., Y., Interaction between projectile driving band and forcing cone of weapon barrel. In: Recent Researches in Mathematical Methods in Electrical Engineering and Computer Science. Angers, Francie: WSEAS Press, 2011, p. 194-199. ISBN 978-1-61804-051-0.

[2] Balla, J., Twin motor drives in weapon systems, *WSEAS Transactions on Systems and Control*, Vol. 5, Issue 9, pp. 755-765, Sept. 2010, ISSN 1991-8763.

[3] DĚL-22-40/4. (Inspections and treatment of the 152 mm Self-propelled howitzer M77. Prague: Ministry of Defence, 1991, (in Czech).

[4] Balla, J., Kinematics and dynamics of ramming devices. *Advances in Military Technology*, Vol. 3, No. 1, 2008, p. 93-104. ISSN 1802-2308.

[5] Balla, J., Duong, V., Y., Krist, Z., Dynamics of shell conveyer with Maltese cross. *International Journal of Mechanics*. NAUN press, Vol. 7, Issue 2, 2013, pp. 81-89. ISSN 1998-4448.

[6] Nepraz, F. Mathematical modelling of hydraulic systems (in Czech). Brno, Military academy, Czech Republic, 1993, 92 pages.

[7] COS 109002 (in Czech). [Translation of STANAG 4517 as Czech Defence Standard Document]. Prague: MoD, 2005. Online: http://www.oos.army.cz/cos/cos/109002.pdf

[8] Next View 4.3 professional software documentation. Maisach (Germany), BMC Messsysteme GmbH, 2009.

[9] Balla, J., Prochazka, S., Beer, S., Krist, Z., Kovarik, M., Jankovych, R. Technical Diagnostics of Tank Cannon Smooth Barrel Bore and Ramming Device. *Defence Science Journal*, 2015, vol. 65, no. 5, p. 356-362. ISSN 0976-464X.

[10] Wu, B.; Zheng, J.; Tian, Q.; Zou, Z.; Chen, X. & Zhang, K. Friction and wear between rotating band and gun barrel during engraving process. WEAR Volume: 318 Issue: 1-2, Pages: 106-113, 2014. doi:10.1016/j.wear.2014.06.020.